Chemistry Europe
European Chemical Societies Publishing

WILEY VCH

Excellence in Chemistry Research

Announcing our new flagship journal

- Gold Open Access
- Publishing charges waived
- Preprints welcome
- Edited by active scientists

Meet the Editors of *ChemistryEurope*

Luisa De Cola
Università degli Studi di Milano Statale, Italy

Ive Hermans
University of Wisconsin-Madison, USA

Ken Tanaka
Tokyo Institute of Technology, Japan

Chemistry–A European Journal
Research Article
doi.org/10.1002/chem.202204010
Chemistry Europe
European Chemical Societies Publishing
www.chemeurj.org

Cyclic or Linear? Parameters Determining the Outcome of Glycine Polymerization in Silica Surface Prebiotic Scenarios

Ola El Samrout,[a, b] Alberto Mezzetti,[b] Gloria Berlier,*[a] and Jean-François Lambert*[b]

Abstract: The parameters that determine the formation of linear peptides and cyclic dimers (diketopiperazine, DKP) on silica surfaces of different surface area, silanol and siloxane ring populations, controlled by thermal treatments, are investigated upon glycine deposition from gas and liquid phases. The formed products were characterized by infrared and Raman spectroscopies, X-ray diffraction and thermogravimetric analysis. The results reveal the importance of "nearly-free" silanols to form ester centers as primers for the formation of linear peptides over DKP, on surfaces with medium silanol density (1.4 to 2.7 nm^{-2}). Quenched reactivity is seen on isolated silanols (density $\leq$ 0.7 nm^{-2}), while silanols involved in hydrogen bonding (density of 4.5 nm^{-2}) weakly interact with Gly resulting in its cyclization to DKP. Deposition of glycine from liquid phase may also form both DKP and linear polymers, depending on its loading and silica surface. These conclusions demonstrate the complexity of glycine surface chemistry in the polymerization reaction and highlight the interest of a surface science approach to evaluate geochemical prebiotic scenarios.

Introduction

The interfacial process between biomolecules and mineral surfaces including silica-based materials is a subject of paramount interest due to its direct implication in promising fields such as bio-nanotechnology,[1] green chemistry,[2] biomedical sensors[3] and peptide-based pharmaceutics.[4] It is also of high importance in the field of prebiotic chemistry where it has long been suggested that mineral surfaces play a key role in the peptide bond formation reaction through the condensation between two amino acids,[5] a critical step in the formation of the first biopolymers on the primitive Earth at the origin of life. To date, several experiments have been carried out to study the amino acid polymerization reactivity on various oxide surfaces, considered as adequate approximations to primordial Earth mineral surfaces. For instance, only a dimerization of glycine (Gly) to linear GlyGly and cyclic diketopiperazine (DKP) with yields higher than 10% was obtained upon heating Gly on TiO_2 at 120 °C for 1–35 days.[6] On alumina, GlyGly was produced along with minor amounts of DKP and triglycine after dry heating of Gly for seven days at 85 °C.[7] DKP has been the major product obtained upon dry heating of Gly on silica, after a selective adsorption procedure (on Aerosil A380),[8–10] or a chemical vapor deposition (CVD) under vacuum at around 200 °C.[11] The cyclic dimer has been also the main product obtained when different amino acids (i.e. Leu, Val, Ala, etc.) other than Gly where deposited from an aqueous phase followed by a single step heating.[12,13] In contrast, only linear poly-Gly chains up to 11 mers were formed using CVD on an amorphous silica Aerosil 50 of a smaller specific surface area.[14]

The existence of diverging results suggests that the nature of the condensation products of amino acids polymerization (linear peptides or cyclic product) on the surface of oxides strongly depends on the reaction conditions, such as the reaction time, the reaction temperature, the deposition method of the adsorbate, the reactive surface sites on the particular type of silica used as a support and the glycine loading.[15] In order to unravel the effect of different factors, we have chosen to address a specific (oxide) mineral-amino acid combination and to investigate their interaction while systematically varying the reaction conditions. Gly was chosen in this work because it is considered as a reference molecule in many theoretical[16] and experimental[9,14] studies dealing with peptide formation. Amorphous silica, a mineral of high natural abundance, low cost, prebiotic significance, and high importance in many potential nanotechnology applications,[17,18] has been considered as a good candidate to study the amino acid polymerization reaction. The surface of silica is characterized by two main surface functional groups, silanol groups and siloxane bridges. The amount of silanol groups directly depends on the type of the silica and the calcination/activation temperature of the surface, and it determines the hydrophilic/hydrophobic character of the material.[19] However, in contrast to ordered crystalline materials, the surface chemistry of amorphous silica is very hard to investigate. A detailed knowledge of the structure of

[a] *Dr. O. El Samrout, Prof. G. Berlier*
Department of Chemistry
University of Torino
Via P. Giuria 7, 10125 Torino (Italy)
E-mail: gloria.berlier@unito.it

[b] *Dr. O. El Samrout, Dr. A. Mezzetti, Prof. J.-F. Lambert*
Laboratoire de Réactivité de Surface, LRS
Sorbonne Université
Place Jussieu, 75005 Paris (France)
E-mail: jean-francois.lambert@upmc.fr

Supporting information for this article is available on the WWW under https://doi.org/10.1002/chem.202204010

amorphous silica and especially of its surface properties would provide a better understanding of the polymerization reactivity of amino acids.

In the present work, we performed experiments of Gly adsorption on amorphous fumed silica surfaces of different surface areas, and Gly deposition on the surfaces was carried out either from the gas (by Chemical Vapor Deposition, CVD) or from the liquid phase (by Incipient Wetness Impregnation, IWI). For gas phase deposition, the silica materials were thermally pre-treated at variable temperatures while for liquid phase deposition, different concentrations of Gly solutions were used. To elucidate the parameters that determine the nature of the condensation products (linear peptides or cyclic ones), several techniques including transmission Fourier transform infrared (FTIR) spectroscopy, attenuated total reflection (ATR-IR) spectroscopy, Raman spectroscopy, thermogravimetric analysis (TGA), X-ray diffraction (XRD), and N_2 physisorption were employed. In particular, we attempt to clarify the role of the different functional groups of silica in the polymerization reaction.

Results and Discussion

Three types of fumed silica surfaces (Aerosil A50, A200, and A380) were used to study the product of the polymerization reaction of Gly when deposited from gas and liquid phases. In the former case, the silica supports were treated at 450, 700, and 850 °C before Gly deposition, in order to modulate their surface properties (silanol and siloxane concentration and nature) and correlate the surface structure to the changes in reactivity. For the Gly adsorption from the liquid phase, only pristine materials were used since it is expected that the exposure to liquid water would undo much of the thermal transformations by re-hydroxylating the surface.

Gly deposited on silica from the vapor phase

Silica supports

BET and TGA analysis

Specific surface areas of the silica supports measured by applying the BET method to N_2 physisorption isotherms are reported in Table 1. The SSAs remain unchanged for A50 and A200 samples (and close to the nominal values) even after calcination at 700 °C. For A380, a decrease of 11 % is seen after a thermal treatment at 700 °C. A more significant decrease of about 30 % is recorded after a calcination at the higher temperature of 850 °C. This decrease probably results from sintering of the nanometric silica particles.[20]

Thermogravimetric analysis (TGA) was employed as a one-step, fast, and simple method to estimate the OH density on the different silica supports[21] in the pristine form and after the different thermal treatments. The number of silanol groups was estimated from the weight loss between 100 and 800 °C because, for silica, the weight loss occurring before 100 °C is associated to the desorption of the physisorbed water from the surface, while the weight loss between 100 and 800 °C is due to the irreversible condensation of surface silanol groups forming siloxane bonds.[22]

Since almost all silanols in Aerosil-type materials are located on the surface, their amount in a sample is given by the product of the surface area (cf. Table 1) and the surface density. Table 2 lists the silanol surface densities of all samples. It can be seen that the higher the surface area, the higher also the silanol density. This is understandable since the synthesis conditions that cause the most silanol condensation induce both the formation of larger particles by sintering (and thus a low surface area) and a transformation of silanols to siloxanes on the remaining exposed surface. According to Zhuravlev the density of 4.5 silanols per nm^2 observed on untreated Aerosil380 corresponds to a "fully hydroxylated silica surface".[23]

For each support, there is a marked decrease in the silanol groups density upon calcination. On calcined A50, the total amount of silanols becomes too low to be quantified by this technique; A200 and A380 reach silanols densities as low as the untreated A50 after calcination, respectively at 450 and 700 °C.

Raman spectroscopic studies

Raman spectroscopy has been used to understand important structural properties of amorphous silicas at the molecular scale.[24–27] The Raman spectra of the different silica supports (A50, A200, and A380) in pristine form and calcined at 450, 700 and 850 °C are reported in Figure 1 (panels A, B, and C respectively). All spectra are normalized with respect to the 800 cm^{-1} band, whose intensity and shape hardly change with thermal treatment as it corresponds to the LO and TO (longitudinal and transverse optic) network vibrations stemming from the ν_{sym} (Si–O–Si).

Table 1. Specific Surface Area (SSA_{BET}) of silica samples (A50, A200, and A380) in the pristine form and after calcination in air at 450, 700 and 850 °C for 2.5 h each. The values are expressed with an experimental error of ±5 %.

	SSABET [$m^2.g^{-1}$]		
sample	A50	A200	A380
pristine	47	197	387
calcined at 450 °C	52	195	371
calcined at 700 °C	52	195	343
calcined at 850 °C	–	–	270

Table 2. Number of silanol (OH) groups [nm^2] for silica samples (A50, A200, and A380) in the pristine form and after calcination in air at 450 and 700 °C for 2.5 h each, calculated using thermogravimetric analysis. The values are expressed with an experimental error of ±5 %.

	Number of OH groups [nm^2]		
Sample	A50	A200	A380
pristine	1.4–1.5	2.7	4.5
calcined at 450 °C	not measurable	1.6	2.0
calcined at 700 °C	not measurable	0.7	1.4

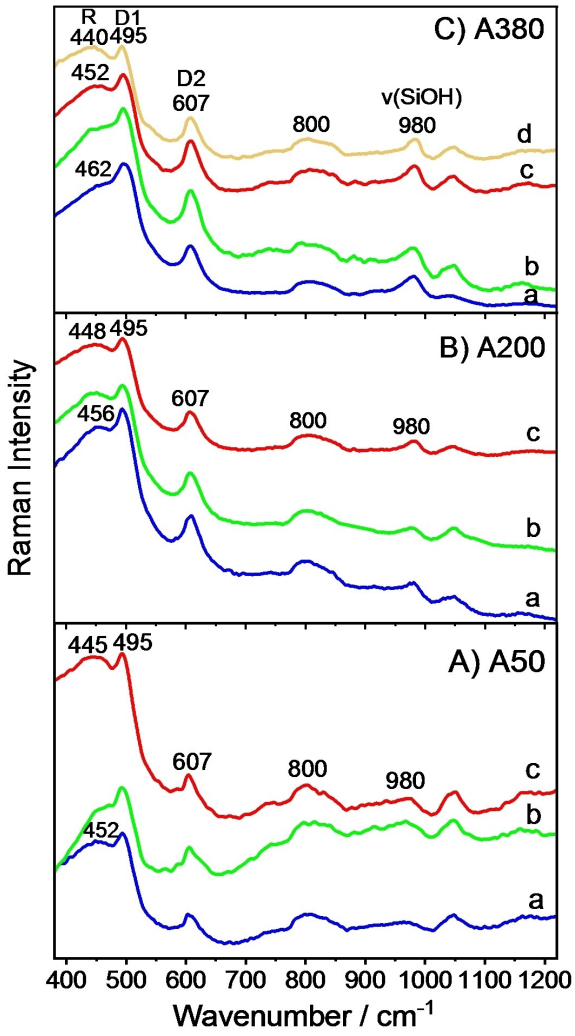

Figure 1. Raman spectra recorded for A) A50, B) A200, and C) A380 silica samples; pre-treated each at different temperatures: (a) rt, (b) 450, (c) 700, and (d) 850 °C for 2.5 h. The spectra are normalized at 800 cm^{-1}, a band characteristic of the silica network.

Different features of silica can be detected from the different spectral Raman bands. The evolution of the silanol groups is seen in the 960–990 cm^{-1} range corresponding to the Si–(OH) stretching.[28,29] The change in the populations of 4- and 3-membered rings can be followed from the characteristic bands of their breathing vibration modes, respectively located at 495 and 607 cm^{-1} and designated as D1 and D2. The R-band, peaking at around 440 cm^{-1} for bulk silica materials,[24,26] is assigned to the bending motions of the O–Si–O. It is sensitive to changes of the silica structure that are induced by small particle size. The R-band position has been reported to be related to the mean Si–O–Si angle.[30]

Comparing the silica materials in pristine form for each type (Figure 1, curves a), the amplitude of the 980 cm^{-1} band increases in the order A50 < A200 < A380, as expected from the silanol amounts deduced from the TG results. The R-band shifts to higher wavenumbers with the increase of the SSA of silica, as already observed by Alessi et al.[26,27] For a given silica, it shifts to lower wavenumbers as the sample is calcined to higher temperatures.

The change in the Raman spectrum upon calcination is most conspicuous for the silica of highest SSA (A380, Figure 1, panel C). For a better quantification, the integrated areas of D1 and D2 as well as the peak position of the R-band were calculated by fitting the normalized Raman spectra using Gaussian function and are illustrated in Figure S1. In this case, after thermal treatment of the A380 support at 450 °C, an increase in the intensity of D1 and D2 bands is seen, which implies the increase in the number of 4- and 3- membered rings in the system through condensation. When A380 is calcined at 700 °C (Figure 1, Panel C, curve c), an opposite effect is observed as the D1 and D2 bands decrease significantly. Meanwhile, as the activation temperature increases, the R-band shifts significantly to lower wavenumber, its position becoming close to that of A50 or A200 calcined at 450 °C. Since the position of the R-band is related to the mean Si–O–Si bond angle, its shift to lower frequency can be interpreted as a higher mean inter-tetrahedral bond angle. As the distribution of the Si–O–Si bond angles is related to that of the ring sizes, this would correspond to a global shift of the ring size distribution toward larger rings.

When heating silica A380 at 850 °C for 2.5 h, the R-band further shifts to lower frequencies, while only negligible changes are observed in the D1 and D2 bands, or the 980 cm^{-1} band (Figure 1, panel C, curve d).

The overall behavior of A380 at temperatures higher than 450 °C could be explained by the cementing of the silica nanoparticles through the formation of necks between the adjacent particles.[20] At the molecular level, silanol groups on originally separated nanoparticles would fuse together, causing the formation of new, rather large rings. Recall that at 850 °C, a 30% decrease in the SSA was observed (Table 1). This is probably due to a decrease in the interparticular porosity related to particle growth; but Raman spectroscopy suggests that this phenomenon starts before noticeable changes in the surface area can be detected.

A similar behavior is also seen on A200 (Figure S1). The trend is less clear on A50, where the D1 and D2 bands were less intense to begin with.

ATR and transmission spectroscopic studies

IR spectroscopy can provide complementary information with respect to Raman, due to the different selection rules of the two spectroscopies. In particular IR in the ATR mode has been used to study the structural and surface properties of silica.[31] ATR-IR measurements (Figure 2) along with transmission measurements (Figure S2) on KBr-IR pellets were carried out on the silica supports in pristine form and after the thermal treatments.

The spectra in Figure 2 exhibit several characteristic bands at around 1188, ~1100, ~800, ~450 cm^{-1} assigned to the LO and TO network vibrations stemming from the ν_{asym} (Si–O–Si) ($\nu_{asym(LO)}$ and $\nu_{asym(TO)}$) LO and TO from symmetric stretching ν_{sym}, and bending δ motions respectively of the Si–O–Si bonds. Furthermore, an additional band can be observed at around

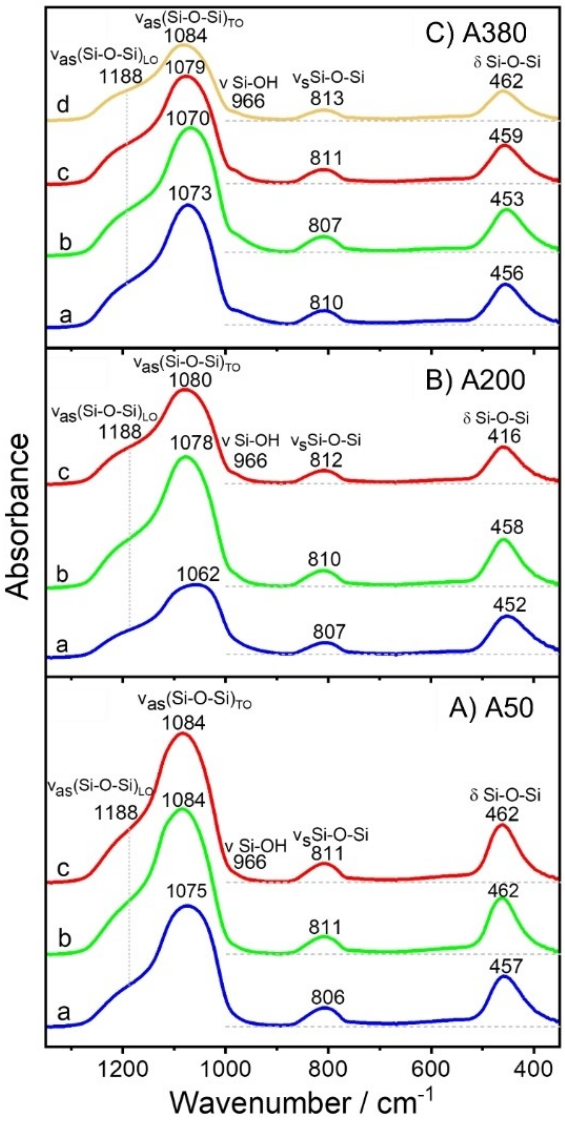

Figure 2. ATR-IR spectra for A) A50, B) A200, and C) A380 silica samples, pretreated at different temperatures: (a) rt, (b) 450, (c) 700, and (d) 850 °C for 2.5 h.

966 cm^{-1} associated to the Si–(OH) stretching of silanol groups.[28,29,31]

The high polarity of Si–O bonds results in an intense absorption band in the 1300–1000 cm^{-1} region from which can be derived the inter-tetrahedral Si–O–Si bond angle.[32] Many previous studies[33–36] have extensively related mainly the TO adsorption band of ν_{asym}(Si–O–Si) and δ(Si–O–Si) to the bond angle of inter-tetrahedral Si–O–Si bonds. They have indicated that a shift to lower wavenumber is indicative of the formation of smaller rings. In our case, both ν_{asym}(Si–O–Si) and δ(Si–O–Si) bands exhibit a redshift along with a decrease in the band associated to νSi–(OH) upon thermal treatments for all the silica supports and especially for the A380 support, which is consistent with the results discussed for Raman spectroscopy (Figure 1). This implies an increase in the mean Si–O–Si bond angle, and consequently the formation of bigger ring structures in the network.

Gly reactivity on silica

XRD analysis

The three types of fumed silica surfaces (Aerosil A50, A200, and A380) were used to study Gly deposition from the gas phase. The XRD patterns of the samples (Figure S3) obtained after 20 h CVD show that no crystalline Gly (or crystalline peptide) is present on the surfaces: instead, only adsorbed species or chemically bonded[37] without crystalline periodicity are present in all silica-deposited samples.

FTIR spectroscopic studies

After 20 h Gly CVD sublimation under argon flow, all silica samples were subjected to FTIR measurements to discriminate among the condensation products obtained after the polymerization reaction. Difference IR spectra in Figure 3 show that when silica A50 and A200 are initially in pristine form or calcined at 450 °C prior to CVD, both the amide I (1700-1610 cm^{-1}) and amide II (1570–1490 cm^{-1}) bands appear with significant intensities after 20 h Gly sublimation. These two bands are indeed intense in linear peptides, while the amide II band should be absent for symmetry reasons in the cyclic dimers.[9] This implies that linear peptides are formed on G/$A50_{(rt)}$, G/$A50_{(450)}$ (Figure 3, panel A, curves a and b respectively) and G/$A200_{(rt)}$, G/$A200_{(450)}$ (Figure 3, panel B, curves a and b respectively). Bands in the 1400–1450 cm^{-1} range are related to H–C–H bending modes, and are not informative about the nature of the formed products. On the other hand, the band in the 1750–1740 cm^{-1} range has been firmly linked with the formation of ester groups between the peptide chains and the silanol groups on the surfaces. These observations are in line with previously observed behavior on the support A50.[37–39]

However, when the A50 and A200 silicas were calcined at 700 °C (G/$A50_{(700)}$ and G/$A200_{(700)}$; Figure 3, Panel A and B respectively, curves c), the amide I and amide II bands after 20 h CVD exhibited a significant decrease with respect to supports pretreated at lower temperatures and the band related to the surface esters disappeared. Thus, high-temperature pretreatment somehow "quenches" glycine polymerization reactivity on both samples.

On A50, the effect of pretreatment temperature on glycine polymerization kinetics were studied in more detail. Intermediate steps of 2.5 h Gly CVD were applied in a specific IR cell for in situ measurements, as described in our previously published papers (Figure S4).[37,38] The results obtained in this setting are coherent with those obtained after ex situ thermal treatments and displayed in Figure 3. In particular, amide I, amide II, amide A bands and surface esters progressively increase during the 20 h CVD on A50, either untreated (Figure S4, panel A) or pre-calcined at 450 °C (Figure S4, panel B). For A50 pre-calcined at

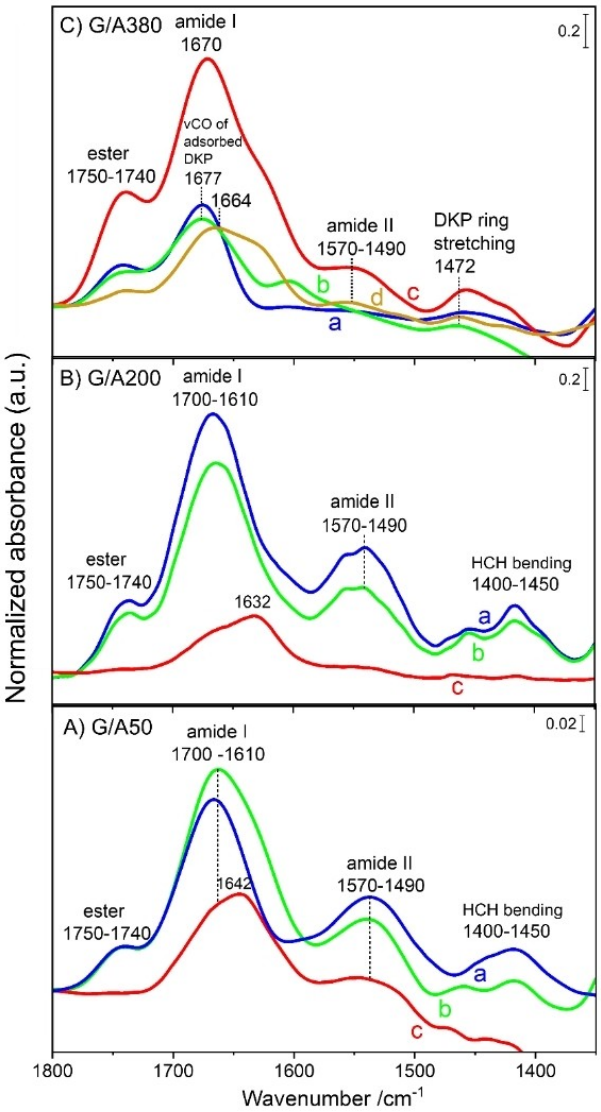

Figure 3. Transmission IR difference spectra measured on self-supporting pellets resulting from Gly deposition by CVD under argon flow for 20 h at 160 °C for the following samples: (A) G/A50, (B) G/A200, and (C) G/A380; in each panel, supports were pre-treated at different temperatures: (a) room temperature (rt), (b) 450, (c) 700, and (d) 850 °C for 2.5 h.

700 °C (Figure S4, panel C), the amide bands are significantly smaller and appear more slowly: only traces are formed after 10 h CVD, even though a small ester band is already present. The cyclic dimer DKP (diketopiperazine) ring stretching band at 1472 cm^{-1}[42,43] is never observed. These observations in the 1400–1750 cm^{-1} region, are correlated with those in the silanol stretching region (higher wavenumbers panels, A′, B′ and C′). Here, negative difference signals indicate that specific types of silanols are consumed during Gly CVD. On A50, untreated (Figure S4, panel A′) or calcined at 450 °C (Figure S4, panel B′), these are specifically the "nearly-free silanol" (NFS) groups, i.e. pairs of silanols separated by a distance between 4 and 6 Å, and absorbing in the 3744–3741 cm^{-1} range.[40] It has been reported that calcination of silica A50 at 700 °C results in the condensation of the NFS groups so that only isolated silanol groups remain on the surface.[41] Indeed, Gly CVD on G/$A50_{(700)}$ does not cause a negative difference signal in the NFS region, but instead a sharp one at 3748 cm^{-1}, a position characteristic of isolated silanols (Figure S4, panel C′). These NFS groups were already highlighted in our previous work[37] as being crucial partners for monomers activation for the polymerization reaction. The results of Figure S4 confirm and specify this hypothesis. Isolated silanols may serve as sites for Gly ester formation; but efficient polymerization from the latter necessitates the presence of NFS.

The relative amount of peptides may be evaluated from the integrated area of the amide I band (Figure S5 in Supporting Information). For all three samples (G/$A50_{(rt)}$, G/$A50_{(450)}$, and G/$A50_{(700)}$, the temporal evolution of peptide bands for G/$A50_{(rt)}$ and G/$A50_{(450)}$ can be roughly fitted with straight lines. On G/$A50_{(450)}$, peptides are significantly more abundant than on G/$A50_{(rt)}$ for the same time of Gly sublimation, with G/$A50_{(700)}$ showing the smallest amounts. Thus, the sample with a support A50 pretreated at 700 °C is the least efficient platform for peptide formation and growth.

For A380 silica-supported samples (Figure 3, panel C), a totally different scenario was observed. When the A380 surface support was untreated or calcined at 450 °C prior to CVD, only an amide I band was observed, shifted to higher wavenumber (1677 cm^{-1}) as compared to polyglycine, with no amide II band (G/$A380_{(rt)}$ and G/$A380_{(450)}$ samples; Figure 3, panel C, curves a and b respectively). There is however a band at around 1472 cm^{-1}, that is not observed for the other silica supports. These features are characteristic of the cyclic dimer DKP.[42,43] This implies that in these two cases, mostly DKP instead of linear peptides was formed on the surface. However, when A380 had been calcined at 700 °C, amide I (now at a lower wavenumber, around 1670 cm^{-1}) and amide II (1570–1490 cm^{-1}) bands were observed with an important growth in the ester band, indicating the formation of linear peptides on the surface along with a significant amount of DKP, detected through the band at 1472 cm^{-1} (Figure 3, panel C, curve c). In view of these results, A380 was further subjected to a pre-treatment at the very high temperature of 850 °C. The spectra of G/$A380_{(850)}$ after 20 h CVD (Figure 3, panel c, curve d) shows the formation of amide I and amide II bands despite their decreased intensities compared to G/$A380_{(700)}$: linear peptides form in this case as well.

Thermogravimetric analysis

Thermogravimetric analysis has been used in previous studies dealing with amino acids oligomerization on silica supports[44–46] and especially for the Gly/SiO_2 system.[9] It constitutes an accurate tool to trace the transformation of amino acids to cyclic or linear peptides and to evaluate the amounts of adsorbed Gly and peptides on the surface. The derivative thermogravimetric (DTG) patterns of G/A50, G/A200, and G/A380 measured after 20 h CVD on supports either untreated or calcined at 450 or 700 °C are displayed in Figure 4.

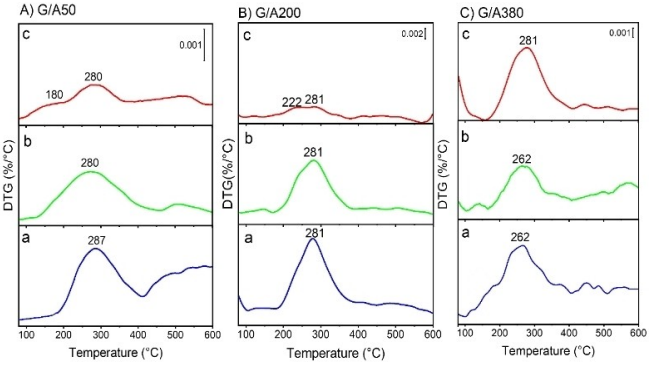

Figure 4. Derivative thermograms (DTG) of samples obtained after Gly sublimation for 20 h by CVD at 160 °C under argon flow on silica: A) G/A50, B) G/A200, and C) G/A380; which supports were pre-treated each at different temperatures: (a) rt, (b) 450, and (c) 700 °C for 2.5 h.

In all cases, physisorbed water desorbs from the surface before 100 °C (not shown). For G/A50 and G/A200, in pristine form or calcined at 450 °C (Figure 4, Panels A and B, curves a and b), a single thermal event is observed at 280–287 °C. Events in this range correspond to the oxidative degradation of the oligopeptides formed on the surface during the CVD.[47] No events are apparent in the 140–160 °C region where peptidic condensation with the loss of water molecules is normally observed.[9,47] This is in keeping with the nature of the CVD products inferred from the IR spectra: whether they consist in DKP or long linear peptides, no or very few free COOH or NH_2 termini are available for condensation anymore.

When A50 and A200 calcined at 700 °C were used as supports (Figure 4, panels A and B, curves c), the peak at ca. 280 °C was barely distinguished along with another event of low intensity in the 180–222 °C range. The latter can perhaps be attributed to the desorption of Gly monomers weakly bound to the surface. The integration of the bands for G/A50 and G/A200 samples reveals that the peptide loadings on $G/A50_{(rt)}$ and $G/A50_{(450)}$ are about 0.27 and 0.37 % by weight of silica respectively while being 1.76 and 1.50 % by weight on $G/A200_{(rt)}$ and $G/A200_{(450)}$, with only traces estimated on $G/A50_{(700)}$ and $G/A200_{(700)}$.

For G/A380, when the support used is in pristine form or calcined at 450 °C, one main peak was observed (Figure 4, panel C a and b) at around 260 °C. This is related to the burning off of the resulting organic matter (consisting of DKP according to IR), at a temperature lower than the one observed in the case of linear peptides.[9] The deposited amounts of DKP constitute about 0.32 and 0.52 % by weight for $G/A380_{(rt)}$ and $G/A380_{(450)}$ respectively. However, when the A380 support is calcined at 700 °C (Figure 4, panel C c), a major event is seen at 281 °C corresponding to an amount of organic matter of 1.19 % by weight. Thus, the TG becomes more similar to those of low temperature-treated G/A50 and G/A200. Recall that IR spectroscopy also indicated a similarity between these same samples, with some linear peptides formed in $G/A380_{(700)}$ (Figure 3, panel C).

The amounts of adsorbed organic matter obtained by TGA are listed for all samples in Table 3, expressed both as bulk loadings and in terms of surface density of Gly monomers. The main FTIR results are also recalled there.

Gly deposited on silica from the liquid phase

XRD analysis

When using the incipient wetness impregnation (IWI) deposition procedure, the weight loading of glycine may be imposed. Different weight loadings ranging from 0.5 (only for A50) to 5 % were deposited on the three different silica samples A50, A200, and A380. After deposition, the samples were activated for 30 min at 160 °C under argon flow. The corresponding XRD patterns after activation are presented in Figure 5 (panels A, B and C for A50, A200, and A380 support respectively). It is expected that the Gly monomers are able to adsorb on the silica surface only up to a maximum surface density known as the saturation coverage. Above the corresponding loading, any additional Gly monomers forced to deposit will precipitate on the surface as bulk Gly.

The XRD patterns of G_x/A50 samples (Figure 5, panel A) do not show any peaks of bulk Gly at low loadings ranging from 0.5 to 3 wt% whereas for 4 and 5 wt%, such peaks appear and grow with Gly loading. As a comparison, a physical (close-

Table 3. Main results obtained from the characterization techniques (FTIR, and TGA) for all the G/SiO_2 samples prepared by Gly deposition from the gas phase. XRD showed the absence of crystalline phases in all samples.

Gly/SiO_2 sample	FTIR	TGA Adsorbed organic matter weight [%]	SiO_2 [mmol Gly/g] (±5 %)	SiO_2 [Gly/nm^2]
G/A50(rt)	linear peptides	0.27	0.04	0.43
G/A50(450 °C)		0.37	0.05	0.59
G/A50(700 °C)	quenched reactivity	traces	.	.
G/A200(rt)	linear peptides	1.76	0.23	0.69
G/A200(450 °C)		1.5	0.20	0.60
G/A200(700 °C)	quenched reactivity	traces	.	.
G/A380(rt)	DKP	0.32	0.04	0.06
G/A380(450 °C)		0.52	0.07	0.11
G/A380(700 °C)	linear peptides	1.19	0.16	0.25

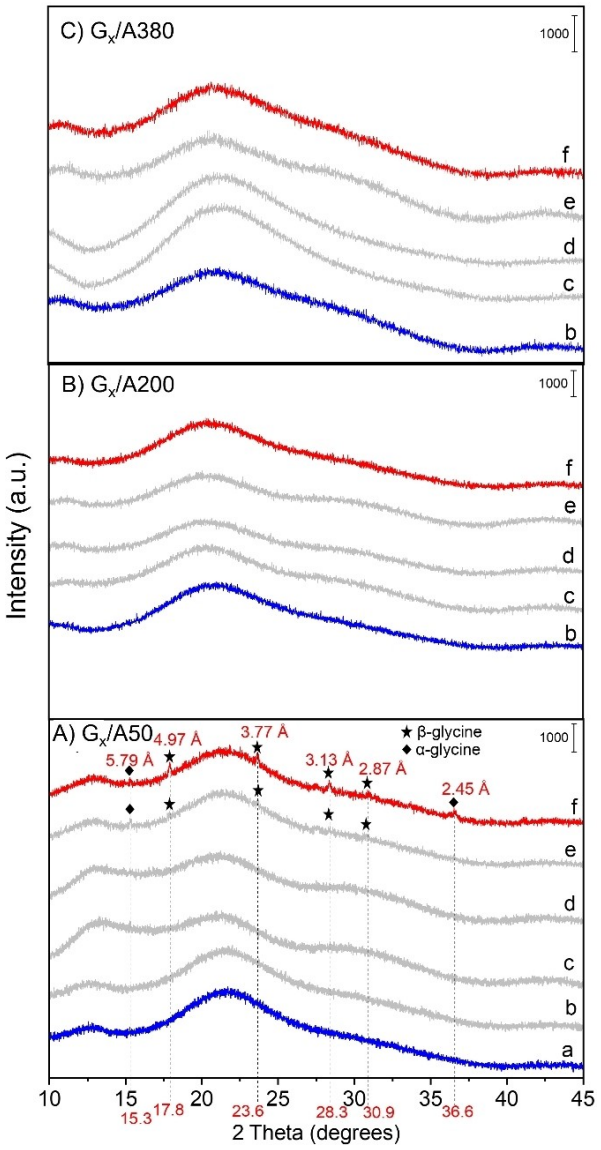

Figure 5. XRD profiles measured after Gly deposition by incipient wetness impregnation followed by activation for 30 min at 160 °C under argon flow on silica: A) G_x/A50, B) G_x/A200, and C) G_x/A380; where *x* refers to different Gly monomers loadings: (a) 0.5, (b) 1, (c) 2, (d) 3, (e) 4, or (f) 5 wt%.

packed) monolayer of Gly (7.3 Gly/nm^2 based on an estimated area of the Gly molecule of 13.65 Å^2[48] (molecules "lying flat" on the A50 surface) would correspond roughly to 4.5 wt% (see Table SI1 where the theoretical value of monolayer coverage may be compared with the surface densities of Gly/nm^2 for all G_x/silica). Most of the XRD peaks observed (2θ equals 17.8, 23.6, 28.3, and 30.9°) may be assigned to bulk β-Gly whereas the ones at 15.3 and 36.6° are associated to α-Gly; this coexistence of the two phases in high-loading samples has been reported before.[9] The observation of bulk monomeric species is also coherent with the fact that bulk glycine does not polymerize at 160 °C, in contrast to silica-adsorbed glycine.[47] For both G_x/A200 and G_x/A380 and for all Gly loadings from 1 to 5 wt%, XRD patterns (Figure 5, panel B and C respectively) only show the broad backgrounds of silica supports without any additional peaks. This implies that all Gly monomers are adsorbed on the surface at least up to 5 wt% without forming any observable crystallites. Indeed, for these samples the 5 wt% loading represents only a fraction of the estimated Gly physical monolayer (around 18 and 35% for A200 and A380, respectively).

FTIR spectroscopic studies

The samples G_x/A50, G_x/A200, and G_x/A380 obtained after Gly deposition by IWI followed by activation at 160 °C for 30 min were investigated by FTIR.

The IR difference spectra of G_x/A50 (Figure 6, panel A) show that at very low Gly loading of 0.5% by weight (curve a), the ester, amide I and amide II bands are formed indicating the formation of peptide bonds on the surface. However, when the Gly loading deposited on the surface increases (for 1 to 5%, panel A, curves b to f), the amide II band is not detected anymore, but instead the DKP ring stretching is observed at around 1473 cm^{-1} indicating the formation of cyclic DKP as a major product on the surface. For curves e and f (panel A) corresponding to 4 and 5% Gly weight loading respectively, additional bands assigned to monomeric Gly appear, which is consistent with the XRD data showing Gly crystallites. These bands probably have a higher extinction coefficient than the amide ones, since they are already predominant in sample G_5/A50, where monomeric Gly accounts for at most 30% of the total deposited glycine. They are located at 1422 and 1528 cm^{-1}, and may be associated to ν_s of COO^- and δ_s of NH_3^+ respectively. As regards the ν_{as} of COO^- and δ_{as} of NH_3^+, they are expected around 1593 and 1606 cm^{-1} respectively, and may overlap with the δ of H_2O adsorbed on silica surface which is located at approximately 1630 cm^{-1}.[49]

For G_x/A200 samples (Figure 6, panel B), the characteristic bands of DKP are predominant from the start, but the amide II band develops with increasing loadings – the ratio of the amide II to DKP breathing bands intensities increases regularly, except for the 3% loading. Thus, while DKP is always the main product, the probability of linear polymer formation increases with the Gly loading. The component around 1630 cm^{-1} related to the water bending mode is apparently weaker with respect to A50.

For G_x/A380 samples (Figure 6, panel C), the samples with the lowest Gly weight loadings (1 and 2%, curves b and c) mostly show the amide I (1683–1673 cm^{-1}), without a noticeable amide II component, and the DKP ring breathing bands (1473 cm^{-1}): DKP is thus the major product. The component assigned to physisorbed water at 1630 cm^{-1} is particularly evident on the low loading sample. As the Gly weight loading increases (3, 4, and 5%), the amide II band (1560–1545 cm^{-1}) becomes conspicuous – this trend is clearer than in the case of G_x/A200.

To summarize, when glycine is deposited from the aqueous phase (IWI procedure), DKP is the main product of thermal condensation on the low-surface A50 support, and also on the higher-surface A200 and A380 when the glycine loading is low,

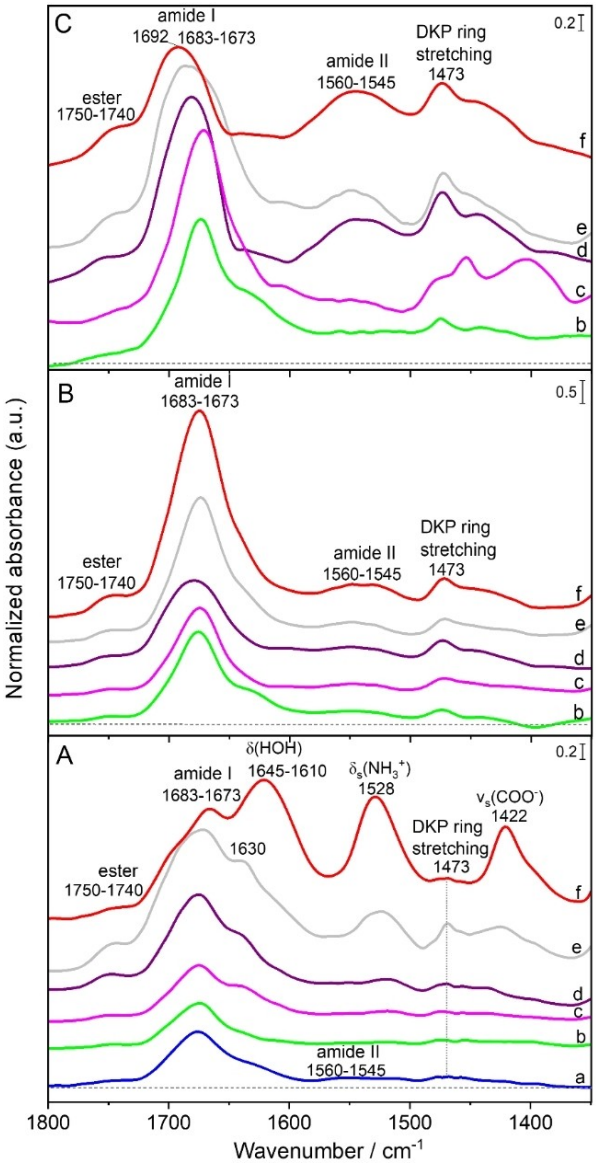

Figure 6. Transmission IR difference spectra measured on self-supporting pellets after Gly deposition by incipient wetness impregnation followed by activation for 30 min at 160 °C under argon flow on silica: A) G_x/A50, B) G_x/A200, and C) G_x/A380; where x refers to different Gly monomers loading: (a) 0.5, (b) 1, (c) 2, (d) 3, (e) 4, or (f) 5 wt%.

while linear polymers are only formed on high-surface supports with high glycine loadings. These findings stand in stark contrast with those obtained for deposition from the gas phase (CVD procedure), where linear polymers were observed on A50, and DKP predominated on A380.

Thermogravimetric analysis

The DTG traces of two unactivated samples ($G_{2\%}$/A380 and $G_{3\%}$/A380) are presented in the Supporting Information (Figure S6 and Table S2). In agreement with previously published data, they exhibit a first, endothermal peak at 137–139 °C, previously shown to correspond to the elimination of water upon amide bond formation, and a second, exothermal event with a first maximum above 250 °C, corresponding to the oxidative degradation of the condensation products. The total integrated values of the two events are in good agreement with the initially deposited glycine amounts, confirming that the thermal events are correctly attributed to Gly and the products of its transformation. However, the intensity ratio of the first to the second peak is higher than the value expected if the first one was exclusively due to amide condensation, especially for the $G_{3\%}$/A380 sample (38 against 24 %). It has been previously observed that when deposited at high surface densities, part of the glycine sublimates instead of condensing.[47] Thus, even if the glycine loading after deposition and drying is known in the IWI procedure, it may be significantly decreased after thermal activation.

Considering now the DTGs of the samples activated at 160 °C (Figure 7), it is expected of course that no thermal events at temperatures lower than this value should be present, and that is what we observed experimentally. Indeed, all G_x/A200 and G_x/A380 samples (Figure 7, panels B and C respectively), as well as the low-loading G_x/A50 (Figure 7, panel A), only show exothermic events starting at 227 °C or higher, previously assigned to the decomposition of glycine polymers. In contrast, the highest-loading G_x/A50 (4 and 5 %) exhibit intense weight losses at 158 and 168 °C respectively, probably corresponding to the sublimation of glycine from the bulk crystallites present in these two samples: similar events have been observed previously for high-loading glycine deposited on Aerosil silica by IWI.[9] G_5/A50 also shows a distinctive peak at 209 °C, perhaps corresponding to the peak at 221 °C in G_4/A50; it may be due to amide condensation in the fraction of the bulk Gly crystallites that have not yet been sublimated.

The decomposition peaks above 200 °C have different fingerprints on A380 and A200, with a single peak at 250 °C in the first case and two components around 220 and 280 °C in the second case. This does not seem to reflect the nature of the polymers, which are similar in both cases according to IR, but perhaps the specifics of their interactions with the two surfaces.

Perhaps more surprising than the DTG profiles is the quantification of weight losses. While the integration of the DTG peaks for unactivated samples gave loadings that corresponded well to the nominal values, the values found after thermal activation were considerably lower, even taking into account the decrease due to condensation water loss (see Figure S7). This means that a considerable proportion of the deposited glycine is lost on sublimation rather than polymerizing (up to 54 % in the highest loading sample). Furthermore, sublimation is confirmed by the observation of cloudy white deposits on the U-cell walls downstream from the sample in the thermal activation step.

General discussion

Thermally induced glycine polymerization on Aerosil-type silicas may result in the formation of linear polymers, cyclic polymers,

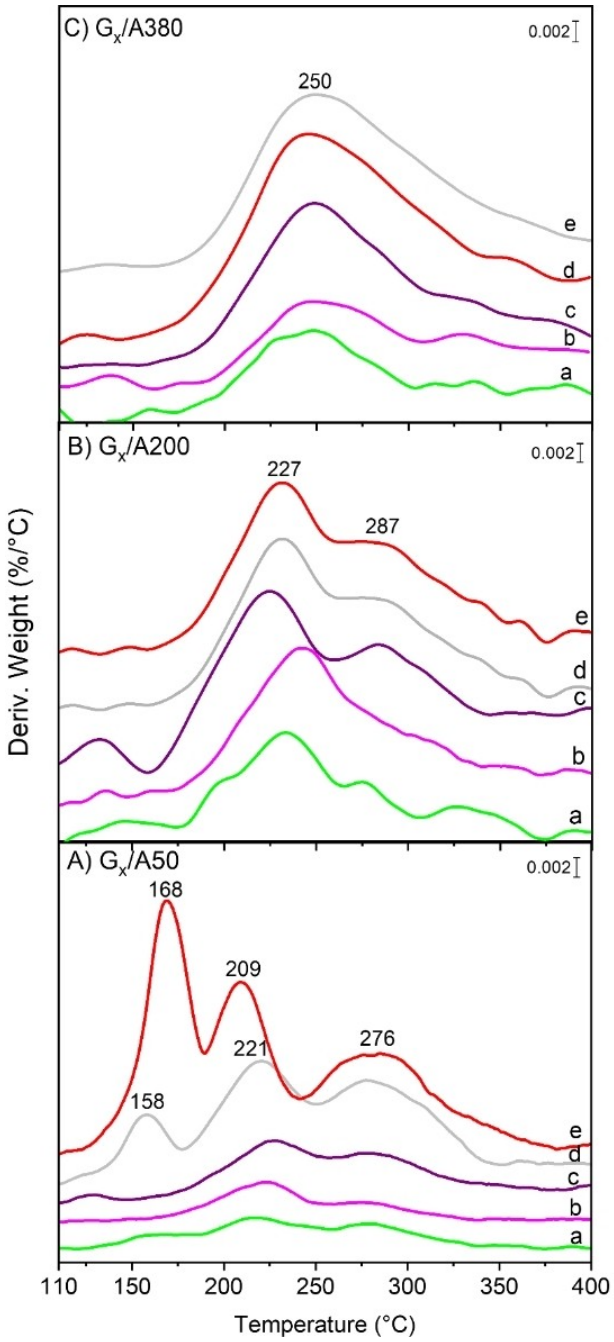

Figure 7. Thermograms (DTG) of samples after Gly deposition by incipient wetness impregnation followed by activation for 30 min at 160 °C under argon flow on silica: (A) G_x/A50, (B) G_x/A200, and (C) G_x/A380; where x refers to different Gly monomers loading: (a) 1, (b) 2, (c) 3, (d) 4, or (e) 5 wt%.

or a mixture of both. The outcome of the polymerization cannot be simply related to experimental parameters. For instance, both types of polymers are found in CVD experiments with deposition of (canonic) glycine from the gas phase and in impregnation experiments, with deposition of (zwitterionic) glycine from the aqueous phase. The distribution is not simply correlated to the density of glycine on the surface either, which is not too surprising since, in the case of linear polymers, the amount of glycine retained depends not only on the chain density, but also on the chain length.

It is probably more promising to consider the possibility that linear polymers formation depends on the presence of particular sites that may exist on the silica surface in certain conditions. These would have to be special combinations of silanol groups and siloxane rings.

One candidate for such sites may be small, strained rings made of 2 to 4 (SiO_4) tetrahedra.[16] We did observe 3-rings and 4-rings by Raman spectroscopy through the D1 and D2 features. Being all of the Aerosil type, our three silica supports did not differ markedly in the amount of 3- and 4-rings – if anything, they were less abundant in A50, that showed ample evidence for linear peptide growth. There was a significant effect of thermal pretreatment of the supports on the D1 and D2 bands. Low-temperature (450 °C) calcination caused an increase in these features, an expected consequence of the condensation of surface silanols.[50] However, calcination at higher temperatures unexpectedly caused them to decrease again. Scheme 1 (Supporting Information) proposes a way in which the condensation of two strained rings might result in the formation of larger rings; if this process happens between strained rings in two different silica particles, it would cause necking, and explain the surface area decrease observed at the highest activation temperature.

At any rate, the amount of strained rings *per se* is not a good predictor of glycine polymerization reactivity: for instance, untreated A380 and A380 heated at 700 °C have about the same densities of 3- and 4-rings (Figure S1), but very different reactivities, as the first one forms mostly DKP, and the second one linear polymers (Table 3).

In contrast, the global silanols density on the surface seems to be correlated with the transformations of glycine. In the CVD procedure, only two samples did not cause significant amide bond formation, namely G/A50(700 °C) and G/A200(700 °C). They were also the only two samples that did not exhibit the band at 1750–1740 cm^{-1} that we assigned to silanol-glycine esters, and the ones with the lowest silanols density ($\leq$ 0.7 nm^{-2}, cf. Table 3). We can surmise that the dearth of silanol groups prevents the interaction of gas-phase glycine with the silica surface, as the molecule does not have any affinity for the siloxane moieties. In contrast, silanol densities in the 1.4 to 2.7 range seem favorable for linear peptide formation; samples with such densities include the pristine A50, which was used in our previous studies.[14,37,38] Gas-phase glycine can be grafted on these surfaces, forming ester groups, and rather long linear peptides grow from these over several tens of hours at 160 °C. Finally, on the sample with the highest density of silanols ($A380_{(rt)}$, 4.5 nm^{-2}), a large amount of DKP is formed (this is still observed on $A380_{(450)}$, with 2 silanols nm^{-2}). In our view, the simplest rationalization of these facts is as follows. A specific type of silanol groups is required to condense with the Gly molecules from the gas phase, providing the primers for growth of the oligopeptide chains. These groups exist in sufficient numbers on silica surfaces with intermediate silanol densities, which therefore constitute the best platforms for linear peptides growth. Surfaces with higher silanols densities contain

in addition other types of silanols that do not form covalent bonds with glycine molecules. They can still activate them, perhaps by strong H-bonding, so that the adsorbed Gly will be activated for reaction with a second Gly coming from the gas phase. Once the Gly-Gly dimer is obtained, it will immediately condense its two free termini to give the cyclic dimer, a reaction that is faster than the initial amide bond formation,[47] yielding the cyclic dimer DKP.

A logical candidate for the crucial, specific surface groups would be the "nearly-free silanols" (NFS), i.e. groups of two silanols separated by a rather large distance (4 to 6 Å) allowing only a weak inter-silanol H-bond. We have demonstrated in a previous paper[37] that these groups play a special role in glycine polymerization. They can form ester groups with Gly, a property shared with isolated silanols; but they also seem to play a specific role in the catalysis of chain elongation, a property that isolated silanols do not share. A previous theoretical study had indeed shown that NFS could have specific properties for the catalysis of amide bond condensation.[41] It is difficult to precisely estimate the density of NFS as a function of the overall silanols density, since the distribution of silanols on the surface is not homogeneous. However, it is logical to think that it should go through a maximum for intermediate silanols coverage, and that at higher silanol densities they should be supplanted by pairs with smaller intersilanols coverage. These different behaviors are sketchily summarized in Figure 8.

Considering now the results of deposition from the aqueous phase. Here the glycine molecules are initially in the form of zwitterions. When the amounts of glycine exceed the saturation coverage, which is close to a physical monolayer, part of the Gly will precipitate separately from the silica surface – this only concerns two samples, G_4/A50 and G_5/A50, that may be excluded from the discussion. For the others, by analogy with other amino acids such as leucine, we expect that a transition to the canonical form will only occur when most or all of the physisorbed water will be eliminated from the surface, at temperatures above 100 °C. At this stage, it seems that a fraction of the Gly does form ester bonds with the NFS (and isolated silanols), as witnessed by the ester bands observed in all IR spectra in Figure 6. The remaining Gly molecules can undergo two different fates, either condensing with the grafted chains to give linear polymers, or with each other to give DKP. If these phenomena were dependent on surface diffusion, it could have been expected that the higher the glycine surface density, the more likely the second fate is, because more concentrated Gly monomers would stand a better chance of meeting each other than of meeting fixed primers. However, exactly the opposite is observed: especially on A200 and A380, DKP predominates for the lowest loadings, while linear peptides are observed for the highest ones.

Therefore, the previous reasoning must contain a flawed assumption. It probably consists in positing that glycine condensation depends on surface diffusion. Diffusion on a dehydrated silica surface at 160 °C is probably slow, but diffusion through the gas phase is an alternate option. Neutral (canonical) Gly molecules formed above 100 °C have a lower adsorption capacity on the silica surface than the initially deposited Gly zwitterions. Therefore, a significant amount of the Gly deposited by IWI desorbs to the gas phase before 160 °C, as amply proved by Figure S7. This gas-phase Gly might then interact with the Gly ester primers on the surface (in an Eley–Rideal type catalytic mechanism), causing the growth of linear oligopeptide chains. This phenomenon would be more significant for the higher-loading Gly samples. In support of this mechanism, it may be noted that an amino acid condensation involving passage through the gas phase has been proposed before,[47] on the basis of a different reasoning.

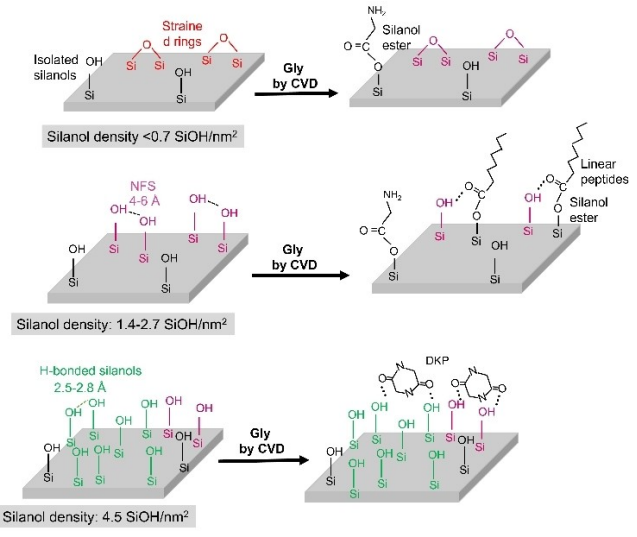

Figure 8. Suggested scheme summarizing the effect of the different types of silanol groups and silanol density present on amorphous silica on the polymerization product obtained.

Conclusion

Amino acids polymerization on silica has been well established for several decades, but previous studies have reported conflicting results as to its outcome, usually without an attempt at justification. In the present work, we have tried to unravel the different factors that determine the formation of cyclic dimers or of linear polymers by comparing several silica supports with different surface areas, varying the surface density of silanol groups by thermal pretreatments, and applying a procedure of deposition from the aqueous phase in addition to the CVD procedure.

In most cases, glycine can form ester bonds with a limited number of silanols on the surface. A subset of these ester centers can act as primers for linear chain growth, as the grafting of one end of the growing chain prevents the otherwise entropically favored peptide cyclization. In agreement with our previous work, we hypothesized that this subset corresponds to the "nearly-free silanols" (NFS) separated a distance of 4 to 6 Å. As the surface silanols density increases, the amount of NFS goes through a maximum (at about 1.5 silanol.nm^{-2} as global silanols density), and the corresponding samples are the most efficient platforms for linear polypeptide

formation. Silica surfaces with much lower silanol densities are inactive; in contrast, surfaces richer in overall silanols contain different pairs that only interact with glycine through weak bonds, so that reaction with an additional Gly from the gas phase results in cyclization to DKP.

Deposition of glycine from an aqueous solution followed by drying may also form both DKP and linear polymers, the latter being observed for high glycine loadings. Surprisingly, a significant amount of glycine desorbs to the gas phase when the samples are activated at 160 °C. Immediately after aqueous deposition, glycine is zwitterionic and may be adsorbed on silica with a rather high saturation coverage close to a physical monolayer; but after dehydration of the surface, it isomerizes to the canonical (neutral) form, which is only retained by the surface in smaller amounts, causing desorption. If enough glycine is desorbed in this way, it will react to the ester primers, forming linear peptide chains.

These results show the complexity of the surface chemistry of amino acids, even the simplest one, glycine. Starkly different outcomes are obtained depending on the glycine deposition procedure, the glycine loading or the thermal pretreatment of the support. Available evidence also suggests that all things being equal, different amino acids can have a different behavior upon thermal activation, as outlined for Val, Leu, Asp and Glu on Aerosil380,[13] highlighting again the need for systematic in-depth studies of prebiotic systems. Obviously, a correct evaluation of the potential of any prebiotic surface scenario necessitates a study of the systems using the concepts and the techniques of materials and surface science. In our case, the elucidation of glycine surface chemistry was based on a combination of IR spectroscopy, Raman spectroscopy, thermogravimetric analysis, X-Ray Diffraction and N_2 physisorption. Solid-state NMR would also be an interesting addition to further studies.

Experimental Section

Materials: Amorphous silicas Aerosil OX 50, Aerosil 200, and Aerosil 380 (designated as A50, A200, and A380) of nominal specific surface areas 50, 200 and 380 $m^2.g^{-1}$ respectively, provided by Evonik (with SiO_2 content $\geq$ 99.8 wt%), were used as supports. Glycine (Gly) (99 %), purchased from Sigma-Aldrich was used as received. Ultrapure Milli-Q water was used for the preparation of the amino acid solution for the liquid phase deposition.

Methods: The silica samples were subjected to different thermal treatments carried out in a muffle furnace. The SiO_2 powder was pressed in the form of a self-supporting pellet before being introduced in the furnace at room temperature (rt), heated with a 30 min ramp up to 450 °C and kept at this temperature for 2.5 h. The temperature was then lowered down to rt. Another set of pellets treated in this way was then ramped for 30 min from 450 °C up to 700 °C, kept at this temperature for 2.5 h, and then left in the furnace to cool down to rt. Only for A380, a fresh pellet previously pre-treated at 450 and 700 °C was further ramped for 30 min to 850 °C, kept again for 2.5 h at this temperature and left to cool down to rt. The supports obtained were labeled as $Ax_{(T)}$, where x represents the specific surface area of the corresponding pristine silica and T refers to the temperature of the thermal treatment.

Gly deposition on the silica surfaces was performed using chemical vapor deposition (CVD) at 160 °C for 20 h. In summary, 200 mg of each silica support (in the pristine form or after thermal treatment), were introduced in a U-shaped cell and placed on its sintered glass bed, with 30 mg of Gly placed upstream in the cell. The system was first subjected to an outgas at rt for 2 h under 100 ml/min argon flow to remove most of the physisorbed water before the start of the reaction. The cell was then placed in a tubular oven controlled by a temperature programmer. A linear temperature ramp of 1 °C/min was applied up to 160 °C and this temperature was kept for 20 h under argon flow, then the sample was left to cool down to rt. The samples obtained after Gly deposition from the gas phase are denoted as $G/Ax_{(T)}$.

For the sake of comparison, a set of pellets of A50 (rt, pre-treated at 450 and 700 °C) were subjected to Gly deposition from the gas phase, also using CVD but performed in an IR cell under vacuum using a method detailed by Martra et al.[14,37]

Gly monomers were deposited on silica surfaces from water solutions using the incipient wetness impregnation (IWI) procedure, derived from the field of supported catalysts synthesis. Briefly, the required amount of Gly monomers were dissolved in ultrapure water and the resulting Gly solution was added to the silica support respecting a ratio of 10 ml of Gly solution for 1 g of silica. This resulted in a homogeneous slurry without a separate liquid phase which was left to dry under nitrogen flow at rt overnight. For each type of silica surface, a series of samples with increasing Gly weight loadings from 0.5 to 5 % was prepared. The different Gly/silica systems were dried under vacuum then introduced in a U-shaped cell for outgas at rt for 10 h under a 100 ml/min argon flow. Subsequently, the U-shaped cell, kept under the same argon flow, was placed in a tubular oven coupled with a temperature programmer for thermal activation of the system. A controlled linear temperature ramp of 1 °C/min was applied to reach a final value of 160 °C where a plateau was maintained for 30 min. The sample was then cooled down to rt and stored in a desiccator. Such samples are labeled as G_y/A_x, where y refers to the Gly weight loading and x represents the specific surface area of the pristine silica used.

IR spectra of the Gly-silica samples were recorded using a Bruker Vertex 80 spectrometer equipped with a MCT detector under a Rapid-Scan mode using a resolution of 4 cm^{-1} and accumulating 250 scans to have a good signal to noise ratio. The samples in the form of self-supporting pellets were placed between two IR-transparent calcium fluoride CaF_2 windows sealed with a parafilm.

KBr-IR spectra for the silica samples (in pristine form or thermally treated at different temperatures) were also recorded in the transmission mode using Bruker Vertex 80 spectrometer (MCT detector, resolution of 4 cm^{-1} with the accumulation of 250 scans). The spectra were measured in potassium bromide KBr pellets with a sample concentration in the pellet of a few percent by weight. The absorption of a pellet of pure KBr was used as a background.

For the samples prepared using the IR cell under vacuum for Gly deposition in the gas phase, IR spectra were recorded using a Bruker Vector 22 instrument with a DTGS detector, using a resolution of 4 cm^{-1} and accumulating 64 scans. The self-supporting pellets of the samples were placed in a traditional IR cell with CaF_2 windows, equipped with a valve to be connected

to a vacuum line (residual pressure $< 1.0 \times 10^{-5}$ mbar) where the adsorption experiments were carried out in situ.

ATR-IR spectra for the silica samples (in pristine form or thermally treated at different temperatures) were recorded using a Bruker Vertex 80 spectrometer equipped with a mono-reflection diamond Bruker, A225/Q-DLST ATR device. The refractive index of the diamond is 2.4. Measurements were carried out with a Rapid-Scan mode using a DTGS detector with a mirror speed of 20 kHz. The spectral window recorded was from 4000–200 cm^{-1} using a resolution of 2 cm^{-1} and accumulating 200 scans for a better signal to noise ratio.

Raman spectra were recorded at rt using a Kaiser microscope optical system (RXN1) equipped with a charge-coupled detector. The laser beam working at 785 nm was focused by adjusting the microscope to an objective of 50X long working distance (8 mm) lens. The spectral window was 3200–150 cm^{-1}; spectra were collected with an incident laser power of 10 mW, resolution of 4 cm^{-1}, 10 seconds acquisition time, and accumulating 30 scans for each spectrum.

Specific surface areas of the silica samples were determined from the N_2 adsorption isotherms recorded at 77 K using Belsorp-max (BEL JAPAN) apparatus. Before measurements, the samples were degassed under vacuum at 250 °C for 2 h (residual pressure 10^{-4} mbar) on a BelprepII-vac unit. Specific areas values were obtained using the BET equation.

XRD patterns for the samples obtained after Gly deposition from gas and liquid phases were recorded on a PANalytical X'Pert powder diffractometer using a Cu Kα ($\lambda = 1.5405$ Å) radiation source generated at 30 mA and 40 kV. The diffractograms were recorded with a 2θ scanning range of 10 to 45°, a step size (2θ) of 0.01°, and a dwell time of 1 s per step.

Thermogravimetric analysis (TGA) of crushed pellets was carried out using a TA instrument with a STD Q600 analyzer. TGAs were performed with a heating rate of 1 °C/min under a 100 mL/min dry air flow. Quantification of adsorbed peptides was evaluated by correcting the weight loss between 130 and 400 °C for the corresponding value for the blank sample.

Acknowledgements

This research acknowledges support from the Project CH4.0 under the MIUR program "Dipartimenti di Eccellenza 2023-2027" (CUP: D13C22003520001). Prof. Piero Ugliengo is acknowledged for fruitful discussions and for suggesting the mechanism of formation of large rings by particles sintering. The authors are grateful to Alice Gava for performing some of the experimental work. Open Access funding provided by Università degli Studi di Torino within the CRUI-CARE Agreement.

Conflict of Interest

The authors declare no conflict of interest.

Data Availability Statement

The data that support the findings of this study are available in the supplementary material of this article.

Keywords: cyclic dimer · glycine · linear peptides · polymerization · silica

[1] R. De La Rica, H. Matsui, *Chem. Soc. Rev.* **2010**, *39*, 3499–3509.
[2] V. R. Pattabiraman, J. W. Bode, *Nature* **2011**, *480*, 471–479.
[3] H. Feyzizarnagh, D.-Y. Yoon, M. Goltz, D.-S. Kim, *WIREs Nanomed. Nanobiotechnol.* **2016**, *8*, 730–743.
[4] K. Fosgerau, T. Hoffmann, *Drug Discovery Today* **2015**, *20*, 122–128.
[5] J. D. Bernal, *Proc. Phys. Soc. Sect. B* **1949**, *62*, 597–618.
[6] U. Shanker, B. Bhushan, G. Bhattacharjee, *Origins Life Evol. Biospheres* **2012**, *42*, 31–45.
[7] J. Bujdák, B. M. Rode, *Alumina Catalyzed Reactions of Amino Acids*, **2003**.
[8] T. Georgelin, M. Jaber, H. Bazzi, J.-F. Lambert, *Origins Life Evol. Biospheres* **2013**, *43*, 429–443.
[9] M. Meng, L. Stievano, J.-F. Lambert, *Langmuir* **2004**, *20*, 914–923.
[10] J. F. Lambert, L. Stievano, I. Lopes, M. Gharsallah, L. Piao, *Planet. Space Sci.* **2009**, *57*, 460–467.
[11] A. Vladimir, T. Y. U. Gromovoy, A. M. Glukhoy, V. G. Golovaty, *Origins Life Evol. Biospheres* **1991**, *21*, 129–144.
[12] C. Guo, G. P. Holland, *J. Phys. Chem. C* **2015**, *119*, 25663–25672.
[13] Y. Sakhno, A. Battistella, A. Mezzetti, M. Jaber, T. Georgelin, L. Michot, J. F. Lambert, *Chem. Eur. J.* **2019**, *25*, 1275–1285.
[14] G. Martra, C. Deiana, Y. Sakhno, I. Barberis, M. Fabbiani, M. Pazzi, M. Vincenti, *Angew. Chem. Int. Ed.* **2014**, *53*, 4671–4674; *Angew. Chem.* **2014**, *126*, 4759–4762.
[15] J.-F. Lambert, *Origins Life Evol. Biospheres* **2008**, *38*, 211–242.
[16] A. Rimola, M. Sodupe, P. Ugliengo, *J. Phys. Chem. C* **2016**, *120*, 24817–24826.
[17] P. Gh Jeelani, P. Mulay, R. Venkat, C. Ramalingam, *Silicon* **2020**, *12*, 1337–1354.
[18] L. Tang, J. Cheng, *Nano Today* **2013**, *8*, 290–312.
[19] A. Comas-Vives, *Phys. Chem. Chem. Phys.* **2016**, *18*, 7475–7482.
[20] G. J. Young, *J. Colloid Sci.* **1958**, *13*, 67–85.
[21] R. Mueller, H. K. Kammler, K. Wegner, S. E. Pratsinis, *Langmuir* **2003**, *19*, 160–165.
[22] S. Ek, A. Root, M. Peussa, L. Niinistö, *Thermochim. Acta* **2001**, *379*, 201–212.
[23] L. T. Zhuravlev, *Langmuir* **1987**, *3*, 316–318.
[24] A. Alessi, S. Agnello, G. Buscarino, F. M. Gelardi, *J. Raman Spectrosc.* **2013**, *44*, 810–816.
[25] B. Humbert, *J. Non-Cryst. Solids* **1995**, *191*, 29–37.
[26] G. Buscarino, V. Ardizzone, G. Vaccaro, F. M. Gelardi, *J. Non-Cryst. Solids* **2011**, *357*, 1866–1870.
[27] A. Alessi, S. Agnello, G. Buscarino, F. M. Gelardi, *J. Non-Cryst. Solids* **2013**, *362*, 20–24.
[28] C. M. Hartwig, L. A. Rahn, *J. Chem. Phys.* **1977**, *67*, 4260–4261.
[29] A. E. Burneau, A., Gallas, J. P., & Legrand, in *Vib. Spectrosc.*, **1998**, pp. 147–234.
[30] B. Hehlen, *J. Phys. Condens. Matter* **2010**, *22*, 10.1088/0953-8984/22/2/025401.
[31] S. L. Warring, D. A. Beattie, A. J. McQuillan, *Langmuir* **2016**, *32*, 1568–1576.
[32] T. Uchino, A. Aboshi, S. Kohara, Y. Ohishi, M. Sakashita, K. Aoki, *Phys. Rev. B* **2004**, *69*, 1–8.
[33] P. Innocenzi, *J. Non-Cryst. Solids* **2003**, *316*, 309–319.
[34] J. Gallardo, A. Durán, D. Di Martino, R. M. Almeida, *J. Non-Cryst. Solids* **2002**, *298*, 219–225.
[35] F. L. Galeener, *Phys. Rev. B* **1979**, *19*, 4292–4297.
[36] F. L. Galeener, A. J. Leadbetter, M. W. Stringfellow, *Phys. Rev. B* **1983**, *27*, 1052–1078.
[37] O. El Samrout, M. Fabbiani, G. Berlier, J. Lambert, G. Martra, *Langmuir* **2022**, *38*, 15516–15525.
[38] O. El Samrout, G. Berlier, J. Lambert, G. Martra, *J. Phys. Chem. B* accepted for publication.
[39] V. A. Basiuk, T. Y. Gromovoy, V. G. Golovaty, *Origins Life Evol. Biospheres* **1990**, *20*, 483–498.

[40] C. Pavan, R. Santalucia, R. Leinardi, M. Fabbiani, Y. Yakoub, F. Uwambayinema, P. Ugliengo, M. Tomatis, G. Martra, F. Turci, D. Lison, B. Fubini, *Proc. Natl. Acad. Sci. USA* **2020**, *117*, 27836–27846.
[41] A. Rimola, M. Fabbiani, M. Sodupe, P. Ugliengo, G. Martra, *ACS Catal.* **2018**, *8*, 4558–4568.
[42] T. C. Cheam, S. Krimm, *Spectrochim. Acta Part A* **1984**, *40*, 481–501.
[43] K. Fukushima, Y. Ideguchi, T. Miyazawa, *Bull. Chem. Soc. Jpn.* **1964**, *37*, 349–353.
[44] Y. Sakhno, A. Battistella, A. Mezzetti, M. Jaber, T. Georgelin Laurentm, J.-F. Lambert, *Chem. Eur. J.* **2019**, *25*, 1275–1285.
[45] H. L. Swanson, C. Guo, M. Cao, J. B. Addison, G. P. Holland, *Phys. Chem. Chem. Phys.* **2020**, *22*, 20349.
[46] C. Guo, J. S. Jordan, J. L. Yarger, G. P. Holland, *ACS Appl. Mater. Interfaces* **2017**, *9*, 17653–17661.
[47] J.-F. Lambert, M. Jaber, T. Georgelin, L. Stievano, *Phys. Chem. Chem. Phys.* **2013**, *15*, 13371.
[48] C. B. Ching, K. Hidajat, M. S. Uddin, *Sep. Sci. Technol.* **1989**, *24*, 581–597.
[49] M. Takeuchi, L. Bertinetti, G. Martra, S. Coluccia, M. Anpo, *Appl. Catal. A* **2006**, *307*, 13–20.
[50] A. Rimola, D. Costa, M. Sodupe, O. Lambert, P. Ugliengo, *Chem. Rev.* **2013**, *113*, 4216–4313.

Manuscript received: December 22, 2022
Accepted manuscript online: February 7, 2023
Version of record online: ■■, ■■

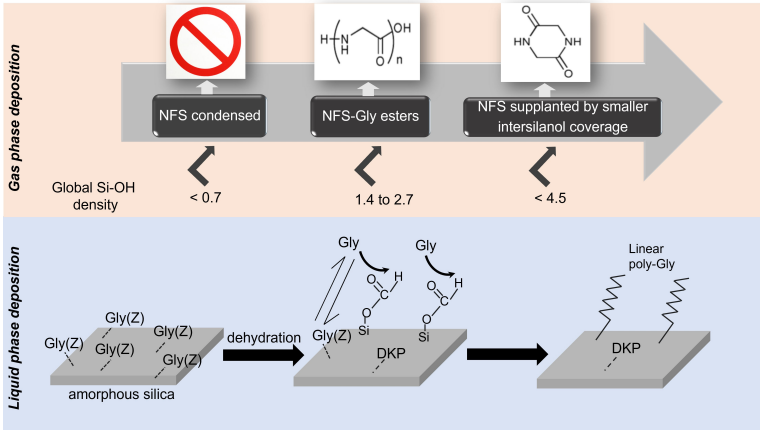

Dr. O. El Samrout, Dr. A. Mezzetti, Prof. G. Berlier, Prof. J.-F. Lambert**

1 – 14

Cyclic or Linear? Parameters Determining the Outcome of Glycine Polymerization in Silica Surface Prebiotic Scenarios

Cyclic or linear? The parameters determining the outcome of glycine polymerization on silica surface are studied through monomers deposition from both gas and liquid phases. The results showed that the density of the nearly-free silanols NFS is a crucial parameter to predict the formation of linear or cyclic polymers when Gly is deposited from gas phase. For liquid phase deposition, Gly deposited in its zwitterionic form could isomerize to its neutral form and readsorb on the silanol-Gly esters to form linear peptides besides DKP.Please consider the following revised version of TOC